JPPIPA 11(6) (2025)

Jurnal Penelitian Pendidikan IPA

http://jppipa.unram.ac.id/index.php/jppipa/index

Utilization of Google Earth Engine and DSAS to Monitor Coastal Change in the Banyuasin Estuary

Heron Surbakti[1,2*], Raisyah Salsabilah[1], Riris Aryawati[1], Isnaini[1], Robinson Sitepu[3]

[1] Department of Marine Science, Faculty of Mathematical and Natural Sciences, Universitas Sriwijaya, Palembang, Indonesia.
[2] Oceanography and Instrumentation Laboratory, Faculty of Mathematical and Natural Sciences, Universitas Sriwijaya, Palembang, Indonesia.
[3] Mathematics Department, Faculty of Mathematics and Natural Sciences, Sriwijaya University, Palembang, Indonesia.

Received: March 19, 2025
Revised: May 15, 2025
Accepted: June 25, 2025
Published: June 30, 2025

Corresponding Author:
Heron Surbakti
heronsurbakti@unsri.ac.id

DOI: 10.29303/jppipa.v11i6.10922

Abstract: This study examines shoreline dynamics in the Banyuasin Estuary, South Sumatra, Indonesia, by integrating multi-decadal satellite imagery (1989-2019) with field-based sedimentation measurements. The research employs Google Earth Engine (GEE) for satellite data processing, FES 2014 tidal corrections to address tidal variations, and the Digital Shoreline Analysis System (DSAS) for precise shoreline change analysis. The primary objective is to comprehensively understand coastline shifts and sediment deposition in stabilising coastal zones. The findings reveal significant shoreline accretion, with net accretion of 2,012 hectares and prominent shoreline advancements at Anakan Island (2,012.33 meters, 118.98 meters/year), while regions such as Sembilang National Park and southern Payung Island exhibited notable erosion (322.71 meters, 10.8 meters/year). The Banyuasin River estuary shifted from notable to extreme accretion phases, contrasting with the more stable shoreline dynamics in the Musi River estuary, where accretion remained stable to intense. The integrated methodology, combining GEE, tidal corrections, and DSAS, offers an innovative approach to monitoring shoreline changes. These findings provide valuable insights for developing sustainable coastal management strategies, particularly in areas facing the dual challenges of climate change and human-induced pressures.

Keywords: Accretion; Banyuasin estuary; Digital shoreline analysis system (DSAS); Google earth engine (GEE); Shoreline change

Introduction

Estuaries are highly dynamic transitional ecosystems between land and sea. They are crucial in maintaining biodiversity and providing vital ecosystem services such as shoreline protection, fish habitat, and carbon sequestration (Dyer, 1997; McLeod et al., 2011; McLusky & Elliott, 2004; Turekian & Holland, 2013). However, these systems are increasingly vulnerable to the pressures of global climate change and human activities, including land-use changes and port development (Nicholls et al., 2021; Vitousek et al., 2017). Understanding the dynamics of shoreline changes and sedimentation in estuarine regions is essential for effective coastal management and environmental protection (Vitousek et al., 2017).

The Banyuasin Estuary in South Sumatra, Indonesia, represents a complex estuarine system shaped by the confluence of the Banyuasin and Musi Rivers. While previous studies have explored shoreline changes and sedimentation patterns in the region (Aritonang et al., 2016; Barus et al., 2020; Surbakti et al., 2011), there is a significant gap in the literature regarding the integration of long-term satellite imagery with field data to comprehensively monitor these processes. Existing research often suffers from limited temporal

How to Cite:
Surbakti, H., Salsabilah, R., Aryawati, R., Isnaini, & Sitepu, R. (2025). Utilization of Google Earth Engine and DSAS to Monitor Coastal Change in the Banyuasin Estuary. *Jurnal Penelitian Pendidikan IPA*, *11*(6), 252–262. https://doi.org/10.29303/jppipa.v11i6.10922

coverage, a lack of systematic tidal corrections, and insufficient incorporation of field measurements into long-term satellite observations, undermining shoreline dynamics modelling accuracy (Surbakti et al., 2011; Handayani et al., 2024b).

Globally, remote sensing technology employing satellite systems has become critical for monitoring coastline changes over vast spatial and temporal scales (Luijendijk et al., 2018; Turner et al., 2021; Vitousek et al., 2017, 2023). However, significant challenges remain, including tidal influences, atmospheric disturbances, and image resolution constraints that limit mapping accuracy (Hoang et al., 2016; Pardo-Pascual et al., 2012; Vos et al., 2019). Studies also indicate that without field validation and application of tidal corrections, estimation errors in shoreline changes may reach 15–25% (Del Río & Gracia, 2013; Eliot & Clarke, 1989; Turner et al., 2021).

This study seeks to address this gap by offering a novel methodology integrating multi-decadal satellite imagery (1989–2019) with sediment trap measurements to monitor coastal changes in the Banyuasin Estuary. The approach incorporates tidal corrections using the FES 2014 model (Vos et al., 2019). Thus, this research overcomes the challenges associated with tidal influences and improves the precision of shoreline extraction. Combining field data with remote sensing techniques provides a more accurate and reliable framework for monitoring shoreline changes over extended periods.

In addition, this study provides new insights into the role of mangrove ecosystems in coastal protection and sediment deposition dynamics. The results demonstrate how mangrove areas contribute to shoreline stabilisation by trapping sediments, significantly influencing sediment accretion in vulnerable coastal regions (Ghufran & Kordi, 2012; Wolanski & Elliott, 2015). These findings underscore the importance of mangrove conservation as a natural barrier to coastal erosion and a key component of sustainable coastal management strategies.

Through this integrated approach, this research makes a significant contribution to the field of coastal monitoring, offering a robust methodology that can be adapted for use in other coastal regions facing similar challenges. Furthermore, the findings of this study provide a comprehensive understanding of shoreline dynamics in the Banyuasin Estuary, offering valuable insights for the sustainable management of estuarine environments and highlighting the critical role of mangrove ecosystems in maintaining coastal resilience in the face of climate change (Vitousek et al., 2017).

Method

Research Location

This study was conducted in the Banyuasin Estuary, located in South Sumatra, Indonesia, where the confluence of the Banyuasin and Musi Rivers creates a complex estuarine environment (Figure 1). The region is characterised by dynamic hydrodynamic conditions influenced by river discharge, tidal processes, and sediment transport. This estuarine system plays a critical role in maintaining local biodiversity and supporting the coastal livelihoods of surrounding communities. The study area was chosen due to its high vulnerability to sedimentation and coastal erosion, which are compounded by human activities such as port development and land-use changes (Y. Handayani et al., 2024; Surbakti et al., 2011). Data processing and analysis were conducted at the Oceanography Laboratory and the Marine Remote Sensing and GIS Laboratory at Sriwijaya University.

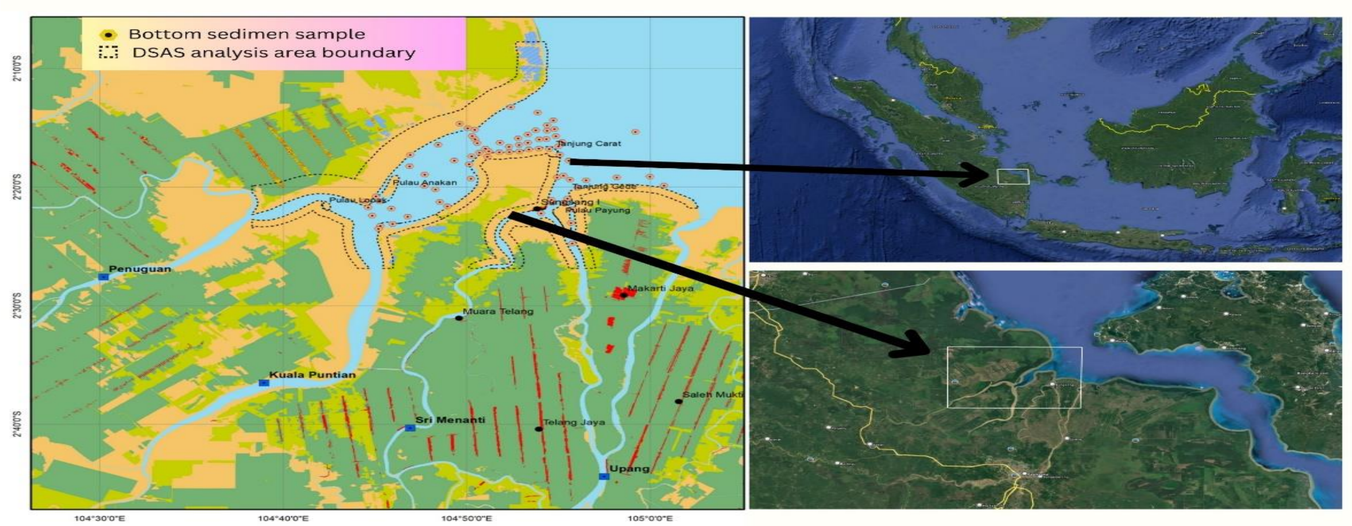

Figure 1. Map of data collection location, bottom sediment, and DSAS analysis area boundary in Banyuasin Estuary

Sedimentation Rate Measurement

Sediment traps were strategically deployed at 12 representative sites within the estuary to measure sedimentation rates (Figure 2). The sites were selected based on factors such as proximity to river mouths, varying hydrodynamic conditions, and areas with suspected high sedimentation rates (Aritonang et al., 2016; Barus et al., 2020; Y. Handayani et al., 2021).

Figure 2. Sediment traps used in the research

Each site was equipped with four PVC sediment traps (5 cm diameter, 11.5 cm height), deployed near the seabed. The traps were replaced weekly, and the collected sediments were dried at 60°C for 24 hours before being weighed. Replicate measurements and oven-drying consistency tests estimated an uncertainty of ±5% in sediment weights. Dry weights were measured to calculate sediment deposition rates expressed in kilograms per square meter per day (kg/m²/day) using the formula adapted from Kozerski (2002):

$$Sedimentation\ rate = \frac{A-B}{sedimen\ trap\ area/week} \quad (1)$$

$$Sedimentation\ rate = \frac{A-B}{\pi.r^2/week} \quad (2)$$

Where A is the weight of aluminium foil + sediment after 105 °C heating (gram); B is the initial weight of aluminium foil after 105 °C heating (gram); π is 3,14, and r is the radius of the sediment trap circle.

Shoreline Change of Banyuasin Estuary

Satellite Data Acquisition

Landsat 5, 7, and 8 images spanning 1989 to 2019 were obtained from the Google Earth Engine (GEE) data catalogue for multi-temporal shoreline analysis. Images with minimal cloud cover were selected to ensure the highest possible accuracy (Gorelick et al., 2017).

Image Preprocessing

Each image underwent geometric correction to improve spatial accuracy and cloud masking to remove cloud cover. Geometry correction is performed using a Digital Elevation Model (DEM) to adjust distortions caused by terrain variations, ensuring accurate alignment of each pixel with real-world coordinates based on elevation data (Dave et al., 2015). Atmospheric correction is applied to mitigate the effects of scattering and absorption in the atmosphere, which can distort satellite imagery and compromise the accuracy of surface reflectance measurements. The atmospheric correction method utilised is Dark Object Subtraction (DOS), which subtracts the radiance of the darkest objects in the scene to compensate for atmospheric interference. Additionally, sensor calibration coefficients correct radiometric distortions, transforming digital numbers into surface reflectance values. This procedure ensures consistency in time series analysis and data comparison across different sensors. These correction steps are executed through automated scripts in Google Earth Engine (GEE), providing an efficient and streamlined approach to processing remote sensing data.

The Modified Normalized Difference Water Index (MNDWI) was applied to extract the shoreline from satellite imagery. MNDWI has been shown to outperform the traditional Normalized Difference Water Index (NDWI) in delineating water from land in estuarine areas (Xu, 2006). The equation used to calculate MNDWI is as follows (Xu, 2006):

$$MNDWI = \frac{(Green-SWIR)}{(Green+SWIR)} \quad (3)$$

Where NDWI is nilai Modified Normalized Difference Water Index; Green is band green (band 2 for Landsat 5 and Landsat 7, and band 3 for Landsat 8); SWIR is band Short Wave Infrared (band 5 for Landsat 5 and Landsat 7, and band 6 for Landsat 8).

Shoreline Extraction

After the initial shoreline delineation, Canny edge detection and Otsu thresholding techniques were employed to refine the boundaries of the shoreline. These methods significantly enhanced the precision of shoreline extraction by reducing noise and improving the clarity of edge detection (Hu & Wang, 2022). The fundamental principle behind this approach involves selecting an optimal threshold value to maximise inter-cluster variance and distinguish between the background and the target object.

The integration of Canny edge detection and Otsu's method for coastline extraction begins by applying Otsu's method, which automatically determines the optimal threshold based on the pixel intensity distribution of the selected band, effectively segmenting the image into two classes: land and water. This segmentation process facilitates identifying foreground (coastline) and background regions. Subsequently, Canny edge detection is utilised to refine the boundaries by highlighting sharp transitions between land and water. The resulting edge map from Canny detection is integrated with the segmented regions obtained from Otsu's method, improving the delineation of the coastline. Finally, morphological operations remove noise and close gaps, ensuring the extracted coastline remains continuous and accurate. This methodology is fully automated using Google Earth Engine scripts, optimising edge detection and image segmentation to achieve highly accurate shoreline extraction.

Shoreline Correction to Tides

Given the significant tidal influence on the study area, tidal corrections were applied to adjust shoreline positions based on tidal heights at the time of satellite overpass. CoastSat is a tool that extracts and measures coastline data from satellite imagery by integrating tidal corrections. CoastSat is an open-source software toolkit written in Python that enables users to obtain a time series of shoreline positions on any coastline worldwide for 40 years (Vos et al., 2019). The tool processes satellite imagery to identify and delineate coastlines, adjusting the shoreline position based on the time of high and low tides.

This correction is applied using the FES 2014 tidal prediction model, which ensures that the shoreline data accurately reflects tidal variations at the time of image acquisition. The shoreline was adjusted per a mean sea level (MSL) reference. Tidal corrections ensure a more accurate representation of shoreline positions and mitigate bias caused by varying tidal stages during satellite image acquisition (Cham et al., 2020). Seasonal and monthly tidal variations were incorporated by applying averaged tidal corrections for each image date, minimising positional bias caused by tidal stage differences. Each shoreline obtained will be shifted towards the sea during high tide and towards land during low tide (Suhana et al., 2017).

Analysis of Shoreline Change

The shoreline corrected with tidal data is then used to analyse shoreline changes and the shoreline's average annual rate of change using DSAS (Digital Shoreline Analysis System) tools. Digital Shoreline Analysis System (DSAS) was employed to calculate shoreline change metrics, including the Net Shoreline Movement (NSM) and the End Point Rate (EPR), to assess the rate of shoreline change over time (Thieler et al., 2009). These methods provide quantitative shoreline accretion and erosion measurements over the past 30 years. This method begins with making transects to determine the size of the shoreline change. The distance of change of each shoreline point is analysed using the NSM method. NSM calculates the total distance of shoreline change by measuring the displacement of shoreline points between the oldest and most recent shoreline positions.

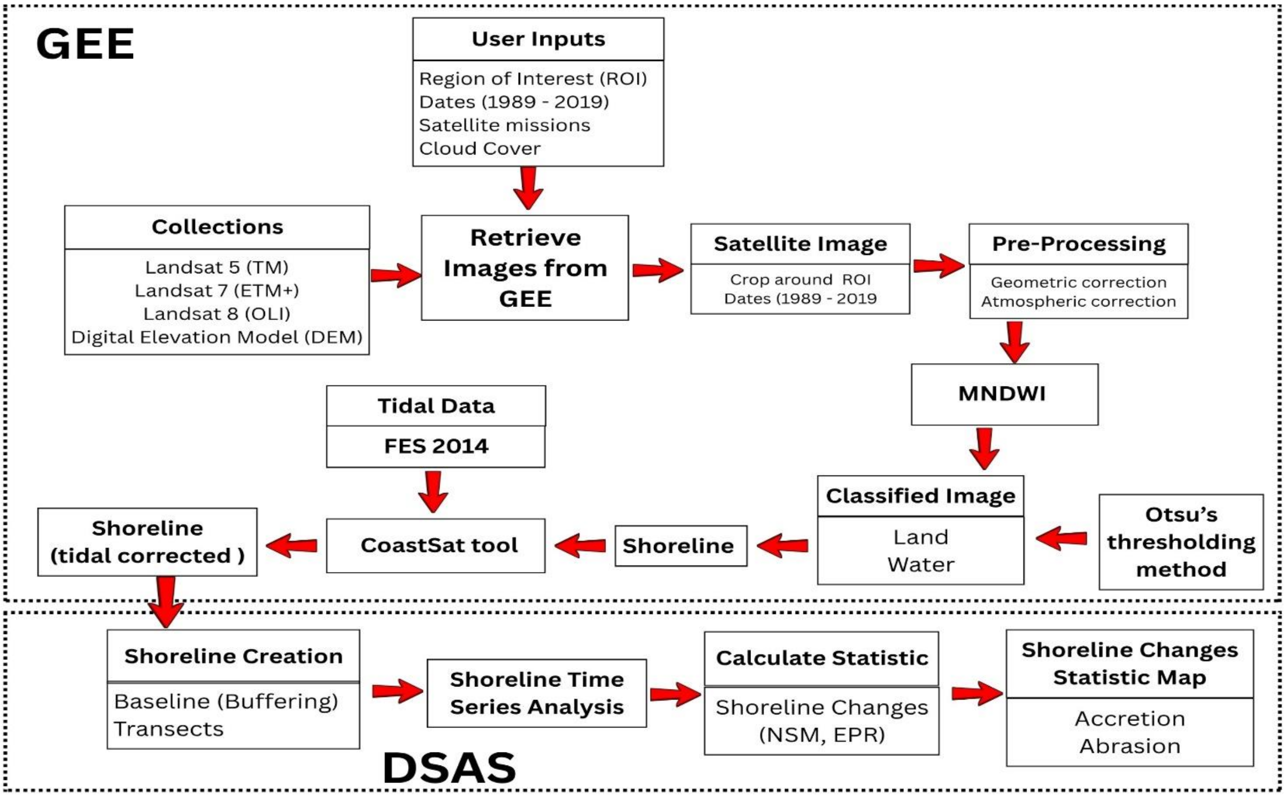

Figure 3. Flowchart of shoreline data processing using GEE and DSAS tools

EPR calculates the average annual rate of shoreline change by dividing the displacement distance by the period in years (Baig et al., 2020; Himmelstoss et al., 2018; Seto et al., 2002; Thieler et al., 2009; Thinh & Hens, 2017). The equation used in the EPR method follows (Thieler et al., 2009):

$$R_{se} = \frac{x_o}{t} \quad (4)$$

Where R_{se} is EPR change (m/year), x_o is the distance of shoreline change (m), and t is the period of shoreline position (year).

Areas experiencing erosion were identified with negative NSM and EPR values, while areas with accretion were identified based on positive values (Seto et al., 2002; Baig et al., 2020). The results of the DSAS analysis reveal the rate and total shoreline change over a specific period. Analysis of shoreline changes using the DSAS method in each transect, where changes of less than 30 meters were categorised as no change because they were smaller than the Landsat image's spatial resolution (30 meters). Figure 3 provides an overview of the entire process of image data processing and coastline change analysis.

Results and Discussion

Sedimentation Rate in Banyuasin Estuary

The sedimentation rates measured at various sites in the Banyuasin Estuary reveal significant variations in sediment deposition across the region (Figure 4). Sediment traps deployed at sites near river mouths, such as the Banyuasin River and Anakan Island, exhibited the highest sedimentation rates. Specifically, the eastern side of the inner Banyuasin River mouth recorded sedimentation rates ranging from 5.59 to 7.31 kg/m²/day, while the western side showed lower rates of 2.56 kg/m²/day. Similarly, the northern part of Anakan Island experienced sediment deposition rates between 2.96 and 5.31 kg/m²/day, while the southern part showed 4.90 and 5.31 kg/m²/day rates. These elevated sedimentation rates can be attributed to the combined influence of river discharge and tidal dynamics, which result in large quantities of sediment deposition in these areas (Aritonang et al., 2016; Barus et al., 2020).

Conversely, areas further inland, such as the Bungin River Estuary and the southern part of Tanjung Api-api, exhibited moderate sediment deposition rates of 2.31–3.88 kg/m²/day and 3.0-5.04 kg/m²/day, respectively. The variation in sedimentation rates reflects the complex interaction of hydrodynamic conditions, sediment properties, and water movement in the estuary (Rifardi, 2008). These results highlight the importance of tidal and river-driven sediment transport in shaping the estuarine landscape.

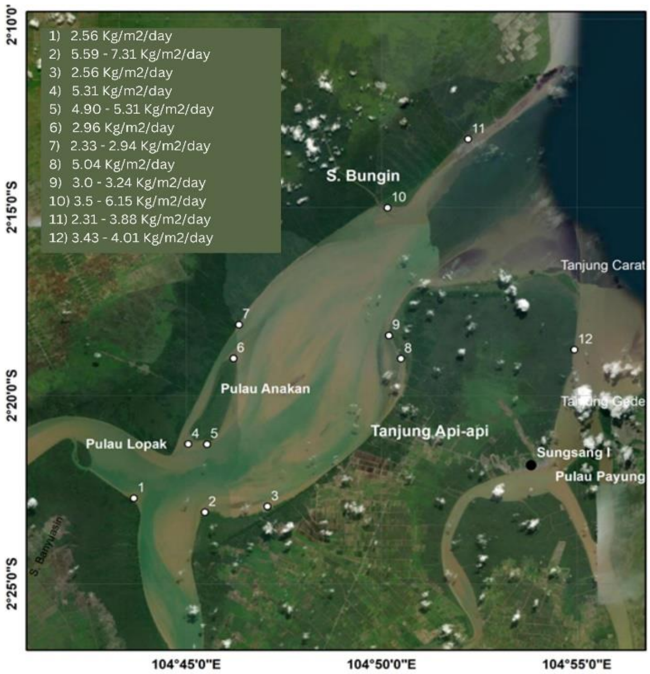

Figure 4. Sediment deposition rate at several locations in the Banyuasin Estuary

Shoreline Change in Banyuasin Estuary

Integrating multi-decadal satellite imagery and field data enabled the detailed analysis of shoreline changes in the Banyuasin Estuary over 30 years (1989–2019). The Google Earth Engine (GEE) platform facilitated the efficient processing of Landsat satellite images, while tidal corrections using the FES 2014 model ensured the accurate representation of shoreline positions. The results revealed that the Banyuasin Estuary experienced shoreline accretion of approximately 2,2,012.33 hectares from 1989 to 2019, with localised erosion totalling 327.92 hectares (Figure 5). Areas experiencing sedimentation are shown in red in Figures 6 and 7 and include Anakan Island, Eastern Banyuasin River Estuary, North of Tanjung Api-api to Tanjung Carat; Bungin River, Banyuasin Peninsula, and Tanjung Gede. Some areas will also experience abrasion in the western Banyuasin River Estuary, from Sungsang to Tanjung Carat, and on the northern and southern parts of Payung Island.

The Net Shoreline Movement (NSM) and End Point Rate (EPR) metrics demonstrated the dynamic nature of the estuarine coastline, with significant variations in shoreline change rates across different regions. Areas like Anakan Island showed substantial shoreline advancement, with maximum shoreline movement reaching 2,012.33 meters over 30 years and an EPR rate of up to 118.98 m/year. A significant shift also occurred between S. Banyuasin and Tanjung Api-Api, where the shoreline moved as far as 1,998.5 meters over three decades, with a net shoreline increase rate of 66.62 meters per year. This reflects a period of rapid sediment deposition and coastal expansion in the region, likely driven by the confluence of riverine sediment inputs and tidal processes (Surbakti, 2012). The most minor shoreline changes occurred in the Telang and Payung Island areas within the Musi River Estuary. The magnitude of maximum shoreline change in both locations was 62.72 m and 92.34 m, respectively, with maximum rates of change ranging from 2.09 to 3.08 m/year.

In contrast, abrasion and erosion were most prominent along the Banyuasin Peninsula and the southern part of Payung Island. The EPR values for these regions were negative, indicating a loss of coastline over time. The most significant erosion occurred in the Banyuasin Peninsula, Sembilang National Park area, where the shoreline receded by 322.71 meters at an average rate of 10.8 m/year. Furthermore, the most significant change due to abrasion is observed in the southern part of Payung Island, where the shoreline has changed by 213.83 m between 1989 and 2019. This corresponds to an average change of 1.16 m/year on Payung Island, with a maximum change rate of 7.13 m/year. This erosion is likely driven by tidal forces, wave action, and human interventions such as port development and infrastructure expansion in this area (Vitousek et al., 2023). The erosion in the Banyuasin Peninsula is mainly due to its exposure to sea waves, which increases the likelihood of erosion. On the other hand, the Payung Island area, being close to settlements and shipping routes, faces potential erosion due to human activities, such as infrastructure development and expansion, as well as shipping lane operations. Based on the change analysis results from 1989 to 2019, the Anakan Island area has not experienced changes due to abrasion. The area experiencing minor abrasion is in the Banyuasin River area to Tanjung Api-api, with a change of 40.86 m, and the rate of change due to abrasion can reach 1.36 m per year. An overview of the changes that have occurred at each location due to accretion and abrasion is shown in Table 1. The results of the shoreline change analysis show that the Banyuasin River Estuary region experienced the most significant shoreline change due to accretion compared to the Musi River Estuary.

Further analysis was conducted to see the phase of shoreline change, referring to the classification of beaches based on the annual shoreline change rate value (Luijendijk et al., 2018). The classification results are shown in Table 2. The analysis of shoreline changes around the Banyuasin River estuary between 1989 and 2029 reveals a clear trend towards the severe accretion to extreme accretion phase, as indicated by the high EPR (Erosion/Accretion Rate) values, ranging from 4.57 to 23.9 meters per year. These positive and significant EPR values suggest substantial sediment accumulation along the coastline. This intense accretion is influenced by factors such as the high sediment discharge from the Banyuasin and Lalan Rivers and the limited water circulation in the area, leading to material deposition along the shore (Affandi & Surbakti, 2012). Additionally, human activities such as coastal infrastructure development may further enhance the accretion process in this region (Luijendijk et al., 2018).

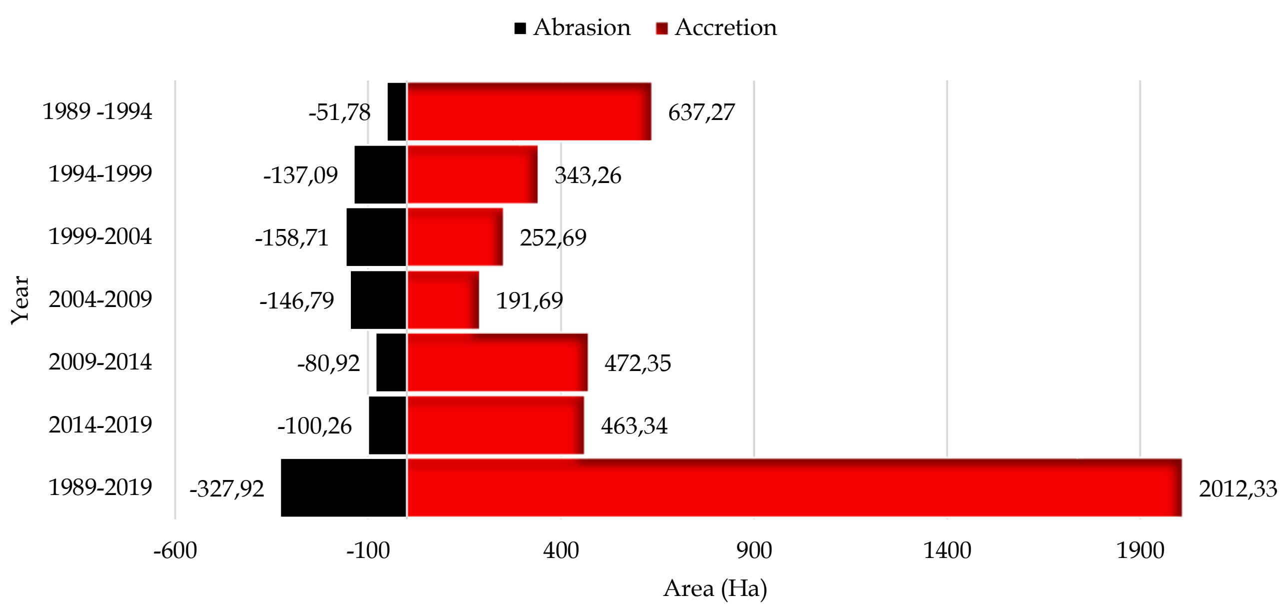

Figure 5. Changes in accretion and abrasion area in the Banyuasin Estuary

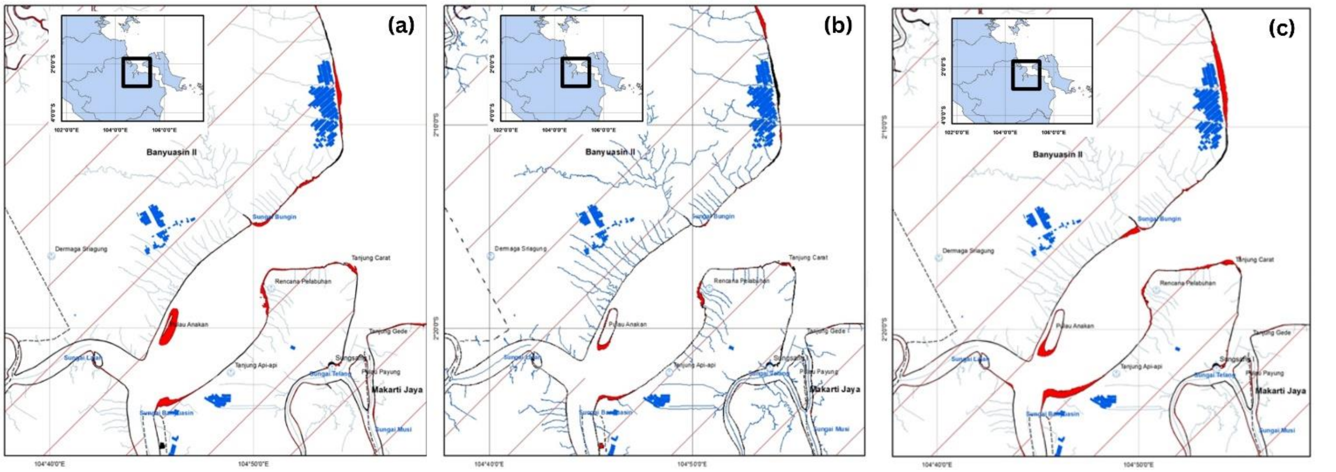

Figure 6. Shoreline changes that occurred in the Banyuasin Estuary. (a) period 1989 - 1999 (b) period 1999 – 2009, (c) period 2009 - 2019 . The red colour depicts the area that experienced sedimentation

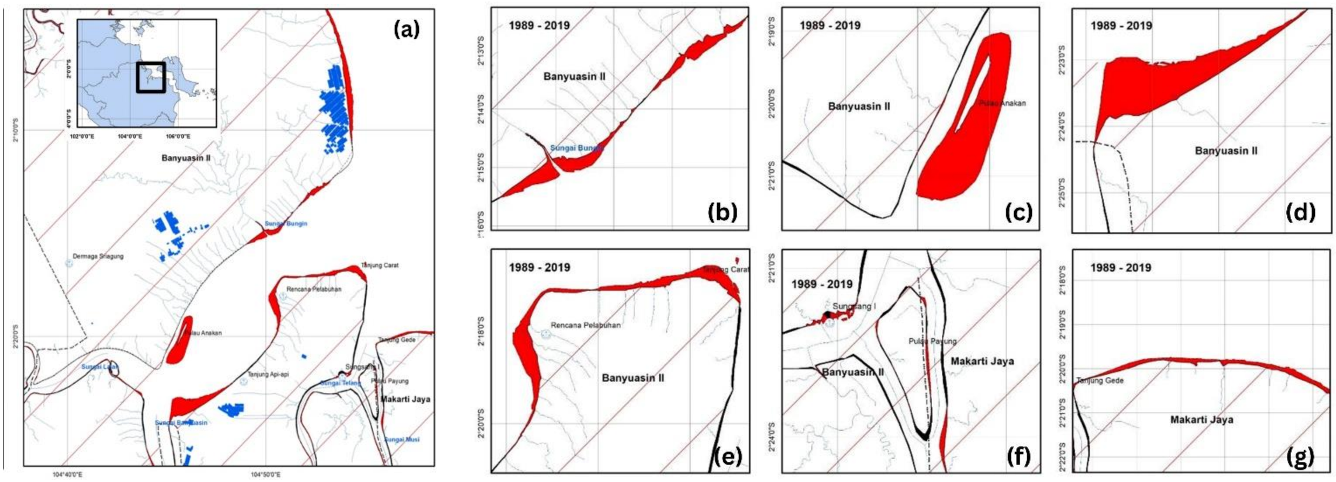

Figure 7. Shoreline changes that occurred in the Banyuasin Estuary from 1989 to 2019. (a) All areas, (b) Bungin River Estuary; (c) Anakan Island; (d) Banyuasin River Mouth; (e) Tanjung Api-api to Tanjung Carat; (f) Payung Island and (g) Tanjung Gede. The red colour depicts areas that experienced sedimentation

Table 1. Shoreline Change, Abrasion, and Accretion Rate in the Banyuasin Estuary from 1989 to 2019

Location	Abrasion				Accretion			
	EPR (m/year)		NSM (m)		EPR (m/year)		NSM (m)	
	Mean	Max	Mean	Mean	Mean	Max	Mean	Mean
Region of Sembilang National Park	-1.35	-10.76	-40.42	-322.71	7.23	31.65	217.00	949.37
Lalan River to Banyuasin River	-0.74	-2.47	-22.07	-74.13	1.99	12.31	59.64	369.30
Anakan Island Area	-	-	-	-	23.90	118.98	435.63	2012.33
Inner Banyuasin River to Tanjung Api-api	-0.71	-1.36	-21.29	-40.86	23.72	66.62	711.61	1998.50
Tanjung Api-Api to Tanjung Carat	-0.85	-1.82	-25.37	-54.74	9.08	27.59	272.37	827.69
Tanjung Carat to Telang River	-1.27	-3.21	-38.08	-96.37	2.11	9.90	63.36	296.97
Telang Area	-0.67	-1.90	-20.01	-57.03	0.77	2.09	23.11	62.72
Payung Island	-1.16	-7.13	-34.91	-213.83	1.11	3.08	33.25	92.34
Tanjung Gede	-1.07	-2.47	-32.00	-74.03	5.74	9.98	120.85	299.43

Table 2. Shoreline Net Change and Classification of the Coast in the Banyuasin Estuary from 1989 to 2019

Location	No	Area	Net change		Classification of the Coast
			EPR (m/year)	NSM (m)	
Banyuasin River	1	Region of Sembilang National Park	4.57	137.01	Severe Accretion
	2	Lalan River to Banyuasin River	4.92	147.53	Severe Accretion
	3	Anakan Island Area	23.9	435.63	Extreme Accretion
	4	Inner Banyuasin River to Tanjung Api-api	23.1	694.26	Extreme Accretion

Location	No	Area	Net change		
			EPR (m/year)	NSM (m)	Classification of the Coast
	5	Tanjung Api-Api to Tanjung Carat	7.6	228.38	Extreme Accretion
Musi River	1	Tanjung Carat to Telang River	-0.5	-16.6	Stable
	2	Telang Area	0.13	4.02	Stable
	3	Payung Island	-0.25	-7.39	Stable
	4	Tanjung Gede	1.9	57.09	Intense Accretion

In contrast, the Musi River estuary shows different shoreline dynamics, where changes are more stable, typically falling within the stable to intense accretion phase. The estuary tends to maintain its shape and equilibrium, with areas experiencing accretion, although it can also undergo erosion due to abrasion (Cui & Li, 2011). The recorded EPR values range from -0.5 to 1.9 meters per year, indicating a balance between erosion and accretion processes, with less sediment accumulation than the Banyuasin River estuary. Although erosion may be more pronounced in certain sections, accretion still occurs at a smaller scale. The limited sediment discharge from the Musi River, combined with stronger hydrodynamic forces, likely explains why this region does not experience intense accretion, resulting in a more balanced interaction between accretion and erosion (Luijendijk et al., 2018; Surbakti, 2012).

The results explain that the extent of coastline changes in the Banyuasin Estuary is suspected to be caused by natural factors such as tides, ocean currents, wave heights, erosion, and accretion (Apriansyah et al., 2019), as well as human factors in the form of land use in the upstream area and the interests of port development, which also contribute to coastline changes (Bidayani & Kurniawan, 2020; S. Handayani et al., 2024; Melo et al., 2024). The changes in coastline occurring in areas experiencing erosion are suspected to be caused by the open coastal characteristics. Waves directly influence this dynamic water characteristic. Coastal regions that protrude into the sea typically experience wave diffraction phenomena and eddy motion, resulting in a more intensive erosion process.

Oceanographic factors significantly influence the sediment transport process in marine waters. The sedimentation process in water is influenced by various water dynamics, including tides, waves, coastal currents, the mixing of water masses due to density differences between freshwater and seawater, and biological and chemical processes. The sedimentation process is also influenced by the properties of the sediments, such as the sediment particles' size, shape, and density (Rifardi, 2008). Weak or low current velocities have a limited sediment transport capacity, resulting in a high deposition rate of deposited particles. The rate of deposition caused by suspended matter is influenced by its physical structure, including volume, particle shape related to sinking direction, density, and porosity (Tomascik et al., 1997). Rifardi (2008) explains that sedimentation is also influenced by the physical properties of seawater, such as density, salinity, and temperature, as well as the hydrological conditions of the area, such as current velocity, shear stress, the vertical position of suspended particulate matter (SPM) in the water column, particle settling velocity, and turbulent mixing.

One of this study's key findings is the significant role of mangrove ecosystems in shoreline stabilisation and sediment deposition. Areas with dense mangrove cover exhibited high sediment deposition rates, particularly in regions such as Anakan Island and the Banyuasin River Estuary (Ulqodry et al., 2021). These findings support previous research showing that mangroves act as natural sediment traps by reducing wave energy and current velocities, thus facilitating the deposition of sediments and promoting shoreline accretion (Ghufran & Kordi, 2012; Wolanski et al., 2011).

The analysis also revealed that mangrove forests along the coastline were instrumental in preventing erosion, particularly in regions with high sedimentation rates. In areas such as the southern part of Anakan Island and Tanjung Api-api, mangrove roots helped to stabilise the soil, preventing sediment from being washed away by strong tidal currents and waves. This highlights the critical role of mangroves in coastal protection and underscores the importance of mangrove conservation in sustainable coastal management strategies (Furukawa & Wolanski, 1996; Jelibseda et al., 2025).

The results of this study provide valuable insights for the sustainable management of estuarine and coastal ecosystems. The findings emphasise the need to consider both natural processes (such as tidal influences and sediment dynamics) and human impacts (such as port development and land-use changes) in coastal management strategies. The observed shoreline accretion in some areas suggests that natural sediment deposition processes are still active and can be enhanced by ecosystem-based solutions, such as mangrove restoration and the protection of wetland habitats (McLeod et al., 2011).

Furthermore, the study's methodology integrates long-term satellite data with field-based sediment measurements and tidal corrections, providing a scalable and adaptable framework for monitoring coastal changes in other regions facing similar challenges. This approach can be particularly valuable for regions experiencing rapid environmental changes due to climate change, sea-level rise, and human activities. By improving the accuracy and reliability of shoreline change assessments, this study supports the development of more effective coastal adaptation strategies.

Conclusion

This study successfully combines long-term satellite imagery, field-based sedimentation data, and advanced analytical methods to track shoreline changes in the Banyuasin Estuary, South Sumatra, Indonesia, over 30 years (1989-2019). The research uses Google Earth Engine (GEE) for satellite data analysis, FES 2014 tidal corrections, and the Digital Shoreline Analysis System (DSAS) to create a comprehensive framework for evaluating coastal dynamics, addressing challenges such as tidal influences. The findings reveal significant shoreline changes, with approximately 2,012 hectares of accretion and notable shoreline advancements in areas like Anakan Island, where the coastline extended by 2,012.33 meters at an average rate of 118.98 meters per year. Conversely, locations like Sembilang National Park and the southern part of Payung Island experienced considerable erosion, with the shoreline retreating by 322.71 meters at 10.8 meters per year. The Banyuasin River estuary showed a clear shift from moderate to extreme accretion, unlike the Musi River estuary, where shoreline dynamics remained relatively stable, fluctuating between stable and intense accretion. This difference in shoreline behaviours highlights the intricate interactions of river discharge, tidal forces, and sediment transport that shape shoreline dynamics in the Banyuasin region. The integrated methodology provides a novel approach for long-term monitoring of shoreline changes and can be adapted for other coastal areas experiencing similar environmental challenges. The study emphasises the importance of sustainable coastal management, focusing on ecosystem-based strategies like mangrove conservation, to bolster coastal resilience against climate change and human impact.

Acknowledgments

The author would like to thank Sriwijaya University for covering this research activity through Decree Number 0013/UN9/LP2M.PT/2024 and research contract Number: 0098.115/UN9/SB3.LP2M.PT/2024

Author Contributions

Conceptualisation and data curation, H.S., R.S., and R.S.; methodology, formal analysis, writing—original draft preparation, and visualisation, H.S., R.S., and R.S.; validation and supervision, R.A., and R.S.; investigation, H.S., R.S., and I.I.; writing—review and editing, H.S., R.A., and I.I. All authors have read and agreed to the published version of the manuscript.

Funding

Sriwijaya University through Decree Number: 0013/UN9/LP2M.PT/2024 and research contract Number: 0098.115/UN9/SB3.LP2M.PT/2024.

Conflicts of Interest

The authors declare that they have no conflict of interest.

References

Affandi, A. K., & Surbakti, H. (2012). Distribusi sedimen dasar di perairan pesisir Banyuasin, Sumatera Selatan. *Maspari Journal*, 33–39. Retrieved from https://www.researchgate.net/publication/263138232_Distribusi_Sedimen_Dasar_di_Perairan_Pesisir_Banyuasin_Sumatera_Selatan

Apriansyah, A., Kushadijayanto, A. A., & Risko, R. (2019). Pengaruh Gelombang pada Perubahan Garis Pantai di Perairan Batu Burung Singkawang, Kalimantan Barat. *Positron*, *9*(1), 1–7. https://doi.org/10.26418/positron.v9i1.32632

Aritonang, A. A., Surbakti, H., & Purwiyanto, A. I. S. (2016). Laju Pengendapan Sedimen di Pulau Anakan, Muara Sungai Banyuasin, Provinsi Sumatera Selatan. *Maspari Journal*, *8*(1), 7–14. Retrieved from https://www.researchgate.net/publication/282630014_Laju_Pengendapan_Sedimen_di_Pulau_Anakan_Muara_Sungai_Banyuasin_Sumatera_Selatan

Baig, M. R. I., Ahmad, I. A., Shahfahad, Tayyab, M., & Rahman, A. (2020). Analysis of shoreline changes in Vishakhapatnam coastal tract of Andhra Pradesh, India: an application of digital shoreline analysis system (DSAS). *Annals of GIS*, *26*(4). https://doi.org/10.1080/19475683.2020.1815839

Barus, B. S., Pratama, M. A. P., & Putri, W. A. E. (2020). Perubahan Garis Pantai di Perairan Muara Banyuasin Kaitannya dengan Sedimentasi. *Jurnal Ilmu Dan Teknologi Kelautan Tropis*, *12*(1). https://doi.org/10.29244/jitkt.v12i1.28276

Bidayani, E., & Kurniawan, K. (2020). Conflict Resolution in Coastal Resource Utilization among Fishermen and Unconventional Tin Miners. *Society*, *8*(1), 13–22. https://doi.org/10.33019/society.v8i1.139

Cham, D. D., Son, N. T., Minh, N. Q., Thanh, N. T., & Dung, T. T. (2020). An analysis of shoreline changes using combined multitemporal remote sensing and digital evaluation model. *Civil Engineering Journal (Iran)*, *6*(1). https://doi.org/10.28991/cej-2020-03091448

Cui, B. L., & Li, X. Y. (2011). Coastline change of the Yellow River estuary and its response to the sediment and runoff (1976-2005). *Geomorphology*, *127*(1–2). https://doi.org/10.1016/j.geomorph.2010.12.001

Dave, C. P., Joshi, R., & S. Srivastava, S. (2015). A Survey on Geometric Correction of Satellite Imagery. *International Journal of Computer Applications*, *116*(12). https://doi.org/10.5120/20389-2655

Del Río, L., & Gracia, F. J. (2013). Error determination in the photogrammetric assessment of shoreline changes. *Natural Hazards*, *65*(3). https://doi.org/10.1007/s11069-012-0407-y

Dyer, K. R. (1997). *Estuaries: a physical introduction*. John Wiley & Sons.

Eliot, I., & Clarke, D. (1989). Temporal and spatial bias in the estimation of shoreline rate-of-change statistics from beach survey information. *Coastal Management*, *17*(2). https://doi.org/10.1080/08920758909362081

Furukawa, K., & Wolanski, E. (1996). Sedimentation in mangrove forests. *Mangroves and Salt Marshes*, *1*(1). https://doi.org/10.1023/A:1025973426404

Ghufran, M., & Kordi, K. M. (2012). *Ekosistem mangrove: potensi, fungsi dan pengelolaan*. Rineka Cipta.

Gorelick, N., Hancher, M., Dixon, M., Ilyushchenko, S., Thau, D., & Moore, R. (2017). Google Earth Engine: Planetary-scale geospatial analysis for everyone. *Remote Sensing of Environment*, *202*. https://doi.org/10.1016/j.rse.2017.06.031

Handayani, S., Zulkarnaini, Z., & Komala, P. S. (2024). Composition of Environmental Parameters in Aquatic Sediments in West Sumatra. *Jurnal Penelitian Pendidikan IPA*, *10*(8), 6170–6180. https://doi.org/10.29303/jppipa.v10i8.7579

Handayani, Y., Ibrahim, E., & Hendri, M. (2024). Coastline abrasion and sedimentation changes on the Banyuasin coast. *Aquaculture, Aquarium, Conservation & Legislation*, *17*(4), 1339–1350. Retrieved from http://www.bioflux.com.ro/docs/2024.1339-1350.pdf

Handayani, Y., Soesanto, R. H., Fauziyah, F., Ibrahim, E., Hendri, M., & Ngudiantoro, N. (2021). Analysis of Sedimentation as Implications of Beach Accretion using Spatial Analysis in the Coastal Area of Banyuasin South Sumatra, Indonesia. *Jurnal Lahan Suboptimal : Journal of Suboptimal Lands*, *10*(2). https://doi.org/10.36706/jlso.10.2.2021.554

Himmelstoss, E. A., Henderson, R. E., Kratzmann, M. G., & Farris, A. S. (2018). Digital Shoreline Analysis System (DSAS) Version 5.0 User Guide. *U.S. Geological Survey Open-File Report 2021–1091*. https://doi.org/10.3133/ofr20181179

Hoang, V. C., Tanaka, H., Mitobe, Y., & Duy, D. Van. (2016). Tidal Correction Method for Shoreline Position Extarcted from Google Earth Images. *Journal of Japan Society of Civil Engineers, Ser. B3 (Ocean Engineering)*, *72*(2). https://doi.org/10.2208/jscejoe.72.i_61

Hu, X., & Wang, Y. (2022). Monitoring coastline variations in the Pearl River Estuary from 1978 to 2018 by integrating Canny edge detection and Otsu methods using long time series Landsat dataset. *CATENA*, *209*, 105840. https://doi.org/10.1016/j.catena.2021.105840

Jelibseda, Kamal, E., Razak, A., & Diliarosta, S. (2025). Analysis of Vegetation Structure and Sustainable Management of Mangrove Forests. *Jurnal Penelitian Pendidikan IPA*, *10*(12), 11239–11248. https://doi.org/10.29303/jppipa.v10i12.9683

Luijendijk, A., Hagenaars, G., Ranasinghe, R., Baart, F., Donchyts, G., & Aarninkhof, S. (2018). The State of the World's Beaches. *Scientific Reports*, *8*(1). https://doi.org/10.1038/s41598-018-24630-6

McLeod, E., Chmura, G. L., Bouillon, S., Salm, R., Björk, M., Duarte, C. M., Lovelock, C. E., Schlesinger, W. H., & Silliman, B. R. (2011). A blueprint for blue carbon: Toward an improved understanding of the role of vegetated coastal habitats in sequestering CO2. In *Frontiers in Ecology and the Environment* (Vol. 9, Issue 10). https://doi.org/10.1890/110004

McLusky, D. S., & Elliott, M. (2004). The Estuarine Ecosystem: Ecology, Threats, and Management. *CEUR Workshop Proceedings*. https://doi.org/10.1017/CBO9781107415324.004

Melo, R. H., Alfin, E., & Niode, A. S. (2024). Water Quality River Estuary of Batang Hari, Musi Banyuasin District, the Province of South Sumatera. *Jurnal Penelitian Pendidikan IPA*, *10*(5), 2860–2870. https://doi.org/10.29303/jppipa.v10i5.6223

Nicholls, R. J., Lincke, D., Hinkel, J., Brown, S., Vafeidis, A. T., Meyssignac, B., Hanson, S. E., Merkens, J. L., & Fang, J. (2021). A global analysis of subsidence, relative sea-level change and coastal flood exposure. *Nature Climate Change*, *11*(4). https://doi.org/10.1038/s41558-021-00993-z

Pardo-Pascual, J. E., Almonacid-Caballer, J., Ruiz, L. A., & Palomar-Vázquez, J. (2012). Automatic extraction of shorelines from Landsat TM and ETM+ multi-temporal images with subpixel precision. *Remote Sensing of Environment*, *123*, 1–11. https://doi.org/10.1016/j.rse.2012.02.024

Rifardi. (2008). Ukuran butir sedimen perairan pantai dumai selat rupat bagian timur sumatera. *Jurnal Ilmu Lingkungan*, *2*(2), 81–88. Retrieved from https://adoc.pub/ukuran-butir-sedimen-perairan-pantai-dumai-selat-rupat-bagia.html

Seto, K. C., Woodcock, C. E., Song, C., Huang, X., Lu, J., & Kaufmann, R. K. (2002). Monitoring land-use change in the Pearl River Delta using Landsat TM. *International Journal of Remote Sensing*, *23*(10). https://doi.org/10.1080/01431160110075532

Suhana, M. P., Nurjaya, I. W., & Natih, N. M. (2017). Analisis Kerentanan Pantai Timur Pulau Bintan, Provinsi Kepulauan Riau Menggunakan Digitas Shoreline Analysis System dan Metode Coastal Vulnerability Index. *Jurnal Teknologi Perikanan Dan Kelautan*, *7*(1). https://doi.org/10.24319/jtpk.7.21-38

Surbakti, H. (2012). Karakteristik Pasang Surut dan Pola Arus di Muara Sungai Musi, Sumatera Selatan. *Jurnal Penelitian Sains*, *15*(1). https://doi.org/10.56064/jps.v15i1.92

Surbakti, H., Purba, M., & Nurjaya, I. W. (2011). Pemodelan Pola Arus di Perairan Pesisir Banyuasin , Sumatera Selatan. *Maspari Journal*, *03*, 9–14. Retrieved from https://www.researchgate.net/publication/263143424_Pemodelan_Pola_Arus_di_Perairan_Pesisir_Banyuasin_Sumatera_Selatan

Thieler, E. R., Himmelstoss, E. A., Zichichi, J. L., & Ergul, A. (2009). DSAS 4.0 Installation Instructions and User Guide. *U.S. Geological Survey Open-File Report 2008-1278*, *3*. Retrieved from https://cmgds.marine.usgs.gov/publications/DSAS/of2008-1278/

Thinh, N. A., & Hens, L. (2017). A Digital Shoreline Analysis System (DSAS) applied on mangrove shoreline changes along the Giao Thuy coastal area (Nam Dinh, Vietnam) during 2005-2014. *Vietnam Journal Of Earth Sciences*, *39*(1). https://doi.org/10.15625/0866-7187/39/1/9231

Tomascik, T., Mah, A. J., Nontji, A., & Moosa, M. K. (1997). *The ecology of Indonesian Seas*. Environmental Management Development of Indonesia (EMDI) and Dalhousie University.

Turekian, K. K., & Holland, H. D. (2013). Treatise on Geochemistry: Second Edition. In *Treatise on Geochemistry: Second Edition* (Vol. 1, Issue 15). https://doi.org/10.1016/C2009-1-28473-5

Turner, I. L., Harley, M. D., Almar, R., & Bergsma, E. W. J. (2021). Satellite optical imagery in Coastal Engineering. *Coastal Engineering*, *167*. https://doi.org/10.1016/j.coastaleng.2021.103919

Ulqodry, T. Z., Aprianto, A. E., Agussalim, A., Aryawati, R., & Absori, A. (2021). Analisis Tutupan Mangrove Taman Nasional Berbak–Sembilang melalui Citra Landsat-8 dan Pemantauan LAI. *Jurnal Kelautan Tropis*, *24*(3), 393–401. https://doi.org/10.14710/jkt.v24i3.12278

Vitousek, S., Barnard, P. L., Fletcher, C. H., Frazer, N., Erikson, L., & Storlazzi, C. D. (2017). Doubling of coastal flooding frequency within decades due to sea-level rise. *Scientific Reports*, *7*(1). https://doi.org/10.1038/s41598-017-01362-7

Vitousek, S., Buscombe, D., Vos, K., Barnard, P. L., Ritchie, A. C., & Warrick, J. A. (2023). The future of coastal monitoring through satellite remote sensing. *Cambridge Prisms: Coastal Futures*, *1*. https://doi.org/10.1017/cft.2022.4

Vos, K., Splinter, K. D., Harley, M. D., Simmons, J. A., & Turner, I. L. (2019). CoastSat: A Google Earth Engine-enabled Python toolkit to extract shorelines from publicly available satellite imagery. *Environmental Modelling and Software*, *122*. https://doi.org/10.1016/j.envsoft.2019.104528

Wolanski, E., & Elliott, M. (2015). *Estuarine ecohydrology: an introduction*. Elsevier.

Wolanski, E., Mazda, Y., & Ridd, P. (2011). *Mangrove hydrodynamics*. https://doi.org/10.1029/ce041p0043

Xu, H. (2006). Modification of normalised difference water index (NDWI) to enhance open water features in remotely sensed imagery. *International Journal of Remote Sensing*, *27*(14), 3025–3033. https://doi.org/10.1080/01431160600589179